Engineering Applications of Artificial Intelligence 71 (2018) 226–235

Contents lists available at ScienceDirect

Engineering Applications of Artificial Intelligence

journal homepage: www.elsevier.com/locate/engappai

An optimum multi-level image thresholding segmentation using non-local means 2D histogram and exponential *Kbest* gravitational search algorithm

Himanshu Mittal *, Mukesh Saraswat

Department of Computer Science & Engineering, Jaypee Institute of Information Technology, Noida, India

ARTICLE INFO

Keywords:
Image segmentation
Multi-level thresholding
Rényi entropy
Gravitational search algorithm
2D histogram

ABSTRACT

Multi-level image thresholding segmentation divides an image into multiple non-overlapping regions. This paper presents a novel two-dimensional (2D) histogram-based segmentation method to improve the efficiency of multi-level image thresholding segmentation. In the proposed method, a new non-local means 2D histogram and a novel variant of gravitational search algorithm (exponential *Kbest* gravitational search algorithm) have been used to find the optimal thresholds. Further, for the optimization, a 2D Rényi entropy has been redefined for multi-level thresholding. The proposed method has been tested on the Berkeley Segmentation Dataset and Benchmark (BSDS300) in terms of both subjective and objective assessments. The experimental results affirm that the proposed method outperforms the other 2D histogram-based image thresholding segmentation methods on majority of performance parameters.

1. Introduction

Image segmentation, the foremost process of image analysis, divides an image into non-overlapping and similar sub-regions. The outcomes of different application areas of computer vision, such as object recognition; object detection; and content-based retrieval, are highly dependent on the efficacy of image segmentation. However, segmenting an object from a complex and coarse image is still a complicated process. Over the last three decades, prevalent segmentation methods have been proposed such as graph-based (Shi and Malik, 2000; Felzenszwalb and Huttenlocher, 2004; Tian et al., 2015), histogram-based (Cheng et al., 2002; Tan and Isa, 2011), thresholding-based (Dirami et al., 2013; Zhang et al., 2015), fuzzy rule-based (Sezgin and others, 2004; Zhang et al., 2008), contour detection-based (Arbelaez et al., 2011), markov random field-based (Mignotte, 2010), texture-based (Krinidis and Pitas, 2009), pixel clustering-based (Yu et al., 2010), and principal component analysis-based (Han et al., 2013). Out of these methods, histogram-based image thresholding segmentation methods are simple and successfully implemented in various application areas.

Image thresholding segmentation can be categorized into bi-level and multi-level segmentation methods based on the number of regions of interest (ROI) in the image. Generally, images contain more than two ROI and hence require multi-level thresholds for segmentation. Further, image thresholding segmentation has also been categorized into six groups by Sezgin and others (2004) on the basis of the information that is used by the methods: histogram-based methods, clustering-based methods, entropy-based methods, object attribute-based methods, spatial methods, and local methods.

The histogram-based methods analyze the one dimensional (1D) histogram information such as peaks, valleys, and curvatures. However, the performances of 1D histogram-based methods are unsatisfactory as they consider the gray level information of an image only and do not deal with spatial correlation among the pixels, an important parameter for segmentation. Therefore, Abutaleb (1989) proposed a 2D histogram-based image thresholding segmentation method where the original gray-level histogram is integrated with local averaging of pixels to form the gray-local 2D histogram. The experimental results of this method are promising in comparison to 1D histogram-based methods. Recently, many researchers used the concept of the 2D histogram for efficient image thresholding segmentation methods (Brink, 1992; Zhao et al., 2016; Sarkar and Das, 2013; Nakib et al., 2007; Ishak, 2017).

Normally, gray-local 2D histogram of an image maps the gray values of the pixels with corresponding local mean values (Abutaleb, 1989; Brink, 1992) to represent the spatial correlation among the pixels. Furthermore, its diagonal plane contains information about the objects and background while the off-diagonal planes carry edge and noise information. Gray-local 2D histogram takes the mean value of a group of pixels surrounding a target pixel to smooth the image due to which the fine details such as points, lines, and edges are blurred (Buades

* Corresponding author.
E-mail addresses: himanshu.mittal224@gmail.com (H. Mittal), saraswatmukesh@gmail.com (M. Saraswat).

https://doi.org/10.1016/j.engappai.2018.03.001
Received 9 August 2017; Received in revised form 27 February 2018; Accepted 1 March 2018
0952-1976/

et al., 2005). As an attempt to consider the edge information, Xue-guang and Shu-hong (2012) proposed a gray-gradient 2D histogram. However, this approach often generates inferior results than gray-local 2D histogram (Sha et al., 2016). Therefore, to include greater post-filtering clarity, this paper proposes a novel 2D histogram based on the non-local means filter. Non-local means filter (Buades et al., 2005; Goossens et al., 2008) calculates the mean of all pixels in the image and is further weighted by the similarity of the pixels with the target pixel.

Moreover, the 2D histogram-based multi-level image thresholding segmentation methods have high computational cost due to the exhaustive search for the optimal thresholds (Otsu, 1979; Kapur et al., 1985). To overcome this problem, meta-heuristic algorithms have widely been employed by the researchers in place of existing derivative-based numerical methods (Zhao et al., 2016; Sarkar and Das, 2013). Meta-heuristic algorithms use the natural phenomena to solve complex optimization problems (Yang, 2014) and are widely used for the image thresholding segmentation (Zhao et al., 2016; Sarkar and Das, 2013; Nakib et al., 2007; Ishak, 2017; Nakib et al., 2010). Differential evolution (DE) (Sarkar and Das, 2013), particle swarm optimization (PSO) (Qi, 2014; Tang et al., 2007; Lei and Fu, 2008), genetic algorithm (GA) (Cheng et al., 2000), simulated annealing (SA) (Fengjie et al., 2009), ant colony optimization (ACO) (Shen et al., 2009), artificial bee colony (ABC) (Kumar et al., 2012), swallow swarm optimization (SSO) (Panda et al., 2017), and artificial fish-swarm algorithm (AFS) (Xiao-Feng et al., 2016) are the meta-heuristic algorithms, used for bi-level and multi-level 2D histogram image thresholding segmentation. According to No Free Lunch theorem (Wolpert and Macready, 1997), no ideal meta-heuristic algorithm exists for all optimization problems and new or existing algorithms can outperform the other for the specific set of optimization problems. This paper focuses on finding an efficacious multi-level image thresholding segmentation method by leveraging the strength of gravitational search algorithm (GSA) proposed by Rashedi et al. (2009).

Gravitational search algorithm (GSA) (Rashedi et al., 2009) is a recently proposed meta-heuristic algorithm based on the concept of Newtonian gravity. In comparison with traditional meta-heuristic algorithms, GSA has performed better in searching the solutions for non-linear functions in multi-dimensional space (Rashedi et al., 2009). GSA uses the collective behavior of objects for finding the optimal solution. Initially, it explores the search space and then exploits it gradually according to Newton's law of gravity and law of motion. Although GSA has the merits of fast convergence rate and low computational cost (Kumar and Sahoo, 2014), it sometimes traps into local optimum and produces poor solution precision (Mittal et al., 2016; Zhang et al., 2012). Therefore, different variants of GSA have been presented in the literature by modifying its parameters like; position (Chatterjee et al., 2012), velocity (Han and Chang, 2012), gravitational constant (Li et al., 2014), and $Kbest$ (Pal et al., 2013). $Kbest$ is one of the important function that maintains the balance between exploration and exploitation in GSA. Generally, it is a linearly decreasing function and defines the number of objects, applying gravitational force at a particular iteration. Hence, it is responsible for the linear transition of GSA from exploration to exploitation (Tsai et al., 2013). Pal et al. (2013) modified $Kbest$ function to enhance the exploitation gradually over exploration after some iterations and solved dynamic constrained optimization problems (DCOP). However, the modified $Kbest$ is also a linearly decreasing function. Recently, chaotic $Kbest$ GSA (cKGSA) (Mittal et al., 2016) has been proposed in which the linear decreasing behavior of $Kbest$ is modified to the chaotic behavior. Although cKGSA shows preferable precision, quick convergence rate, and better global search ability, however, the dependency of chaotic behavior on initial conditions may affect the results (Boccaletti et al., 2000). Therefore, this paper proposes a novel variant of GSA termed as exponential $Kbest$ gravitational search algorithm (eKGSA) in which an exponentially decreasing $Kbest$ has been introduced to intensify the vicinity of search space. Further, the proposed eKGSA has been used to find the optimal thresholds in non-local means 2D histogram-based multi-level image segmentation method.

Moreover, the solution of a meta-heuristic algorithm is dependent on the selection of the optimization (or cost) function (Sarkar et al., 2015). Entropy is a popular cost function, used by meta-heuristic algorithms in multi-level image thresholding segmentation (Akay, 2013; Marciniak et al., 2014). It represents a measure of disorder or randomness in system (Bekenstein, 1973). In an image, homogeneous regions correspond to minimum entropy while non-homogeneous regions define maximum entropy. Therefore, the high entropy of a segmented image represents better separation among regions, thus may serves as an objective function for finding the optimal thresholds. Shannon entropy (Shannon, 2001), Kapur entropy (Kapur et al., 1985), Tsallis entropy (Albuquerque et al., 2004), Cross entropy (Li and Tam, 1998), and Rényi entropy (Renyi, 1961) are widely used entropies in image thresholding segmentation (Sarkar et al., 2015; Albuquerque et al., 2004; Sahoo and Arora, 2004). Abutaleb (1989) compared the use of entropy on 1D and 2D gray-local histograms and observed that the segmentation results using 2D histogram were more accurate than the 1D histogram. Qi (2014) used adaptive PSO and 2D Shannon exponential entropy for performing bi-level image segmentation. Sahoo and Arora (2006) introduced a 2D Tsallis–Havrda–Charvt entropy for image thresholding segmentation. Moreover, Sarkar and Das (2013) used 2D Tsallis entropy and DE algorithm for an automatic multilevel image thresholding scheme. Further, Nie (2015) determined the optimal thresholds for bi-level image segmentation by using a 2D Tsallis cross-entropy. Zhao et al. (2016) proposed an approach that calculates the 2D K–L divergence between an image and its segmented regions by adopting 2D histogram as the distribution function. An image segmentation technique based on 2D Rényi's entropy has been introduced by Sahoo and Arora (2004) in which the work of Sahoo et al. (1997) has been extended. Xiao-Feng et al. (2016) presented a 2D Rényi's entropy using the adaptive artificial fish-swarm algorithm for segmentation of infrared images. Further, due to the complexity of 2D Rényi entropy, Cheng et al. (2014) introduced another image thresholding segmentation method based on 2D Rényi gray entropy and fuzzy clustering where two 1D Rényi entropies were computed for forming 2D Rényi entropy. It has been observed from the literature that Rényi entropy on 2D histogram shows better performance (Xiao-Feng et al., 2016; Cheng et al., 2014), however, it has only been used for bi-level thresholding. Therefore, this paper introduces the multi-level version of Rényi entropy for the 2D histogram.

The overall contribution of this paper has been divided into four folds, (i) a novel 2D histogram has been introduced based on non-local means, (ii) a novel variant of GSA, exponential $Kbest$ gravitational search algorithm (eKGSA), has been presented and used to find the optimal thresholds in 2D histogram, (iii) the Rényi entropy has been redefined for multilevel thresholding on 2D histogram and used as a fitness function for eKGSA, (iv) a two-dimensional non-local means exponential $Kbest$ gravitational search algorithm (2DNLMeKGSA) for multi-level image thresholding segmentation has been introduced. To validate the efficiency of 2DNLMeKGSA, extensive experimental analysis has been done on 300 images from the Berkeley Segmentation Dataset and Benchmark (BSDS300) (The Berkeley Segmentation Dataset and Benchmark, 2017). The results are illustrated for 3-level and 5-level image thresholding segmentations and analyzed in terms of both subjective and objective assessments. The result evaluations are based on human-made image segmentations (Ground Truth) and twelve performance parameters of segmentation namely; boundary displacement error (BDE), probability rand index (PRI), variation of information (VoI), global consistency error (GCE), structural similarity index (SSIM), feature similarity index (FSIM), root mean squared error (RMSE), peak signal to noise ratio (PSNR), normalized cross-correlation (NCC), average difference (AD), maximum difference (MD), and normalized absolute error (NAE).

The rest of the paper is organized as follows: Section 2 briefly introduces non-local means; gravitational search algorithm; and Rényi entropy, required for the proposed method. The proposed method and its mathematical formulation are discussed in Section 3. Section 4 presents the experimental results, analyzed on BSDS300. Finally, the paper is concluded along with future scope in Section 5.

2. Preliminaries

In this section, non-local means, gravitational search algorithm, and Rényi entropy are briefed.

2.1. Non-local means

Non-local means (Buades et al., 2005) computes the weighted average of all the pixels in an image. Let $X(p)$ and $X(q)$ are the respective values of p and q pixels in an image X. The non-local means of X can be computed by Eq. (1).

$$Y(p) = \frac{\sum_{q \in X} X(q) w(p,q)}{\sum_{q \in X} w(p,q)} \tag{1}$$

where, $Y(p)$ is the output value of pixel p and $w(p,q)$ is the Gaussian weighting function defined by Eq. (2).

$$w(p,q) = exp^{-\frac{|\mu(q)-\mu(p)|^2}{\sigma^2}} \tag{2}$$

where, σ is the standard deviation. $\mu(p)$ and $\mu(q)$ are the local mean values at pixels p and q respectively and are calculated using Eqs. (3)–(4).

$$\mu(p) = \frac{1}{m \times m} \sum_{i \in F(p)} X(i) \tag{3}$$

$$\mu(q) = \frac{1}{m \times m} \sum_{i \in F(q)} X(i) \tag{4}$$

here, $F(p)$ is a square filter of size $m \times m$.

2.2. Gravitational search algorithm

Gravitational search algorithm (GSA) (Rashedi et al., 2009) is a meta-heuristic algorithm based on the physical phenomenon of mass interactions. The GSA is based on Newton's law of gravity and law of motion. The algorithm considers each agent as an object and evaluates the performance in terms of masses. Each object applies force in the system according to the law of gravity and changes its position according to the law of motion. The number of objects exerting force at an iteration is represented by $Kbest$ which controls the trade-off between exploration and exploitation. The slower movement of a heavier object corresponds to the exploitation and represents a better solution. The position of the object with the heaviest mass represents the optimal solution of the problem at the end of the stopping criteria.

Consider a system of N objects in u dimensional search space of GSA where the position of each object is depicted by Eq. (5).

$$O_i = (o_i^1, \dots, o_i^d, \dots, o_i^u),\ i = 1, 2, \dots, N \tag{5}$$

here, ${o_i}^d$ denotes the d^{th} dimension of the i^{th} object.

The total force $F_i^d(t)$ in d^{th} dimension of o^{th} object at t^{th} iteration is defined as randomly weighted sum of d^{th} components of the force from other $Kbest$ objects and is shown in Eq. (6).

$$F_i^d(t) = \sum_{j=1, j\neq i}^{Kbest} rand_j {F_{ij}}^d(t), \tag{6}$$

here, $rand_j$ is a random number in the interval [0, 1], F_{ij} is the force of j^{th} object on i^{th} object, and $Kbest$ for the t^{th} iteration is defined by Eq. (7).

$$Kbest(t) = final\_per + \left(\frac{1-t}{max\_it}\right) \times (100 - final\_per), \tag{7}$$

Algorithm 1 Gravitational Search Algorithm (GSA)

Input: N objects having u dimensions. Assume the value of $final\_per$.
Output: The best solution having the heaviest mass.

```
Randomly initialize the initial population of N objects;
Evaluate the fitness (fit) of each object;
Compute the mass M of each object by Eq. (10);
Set Kbest = N;
while stopping criteria is not satisfied do
    Compute the acceleration a of each object by Eq. (8);
    Compute the velocity v of each object by Eq. (13);
    Update the position of each object by Eq. (14);
    Evaluate the fitness fit for each object;
    Compute the mass M of each object by Eq. (10);
    Update Kbest as: Kbest = final_per + ((1−t)/max_it) × (100 − final_per),
end while
```

where, max_it is the maximum number of iterations and $final\_per$ is the percent of objects which apply force on others. Eq. (7) shows that the value of $Kbest$ decreases linearly over iterations.

The calculated force $F_i^d(t)$ is used to find the acceleration of i^{th} object in the d^{th} dimension according to the law of motion as shown in Eq. (8).

$$a_i^d(t) = \frac{F_i^d(t)}{M_i(t)}, \tag{8}$$

where, $M_i(t)$ corresponds to mass of i^{th} object at iteration t and is calculated by Eq. (10).

$$m_i(t) = \frac{fit_i(t) - worst(t)}{best(t) - worst(t)}, \tag{9}$$

$$M_i(t) = \frac{m_i(t)}{\sum_{j=1}^{N} m_j(t)}, \tag{10}$$

where, $best(t)$ and $worst(t)$ are measured by Eq. (11) and Eq. (12) respectively for minimization problem.

$$best(t) = \min_{j \in \{1,\dots,N\}} fit_j(t) \tag{11}$$

$$worst(t) = \max_{j \in \{1,\dots,N\}} fit_j(t) \tag{12}$$

Now, the updated velocity and position of an object are calculated by Eq. (13) and Eq. (14) respectively.

$$v_i^d(t+1) = rand_i \times v_i^d(t) + a_i^d(t), \tag{13}$$

$$o_i^d(t+1) = o_i^d(t) + v_i^d(t+1). \tag{14}$$

As an object's position corresponds to the solution, the heaviest object in the system will be the fittest object and its position will represent the optimal solution of the problem at the end of stopping criteria. The pseudocode of the GSA is presented in Algorithm 1 (Rashedi et al., 2009).

2.3. Rényi entropy

Shannon (2001) states that the amount of information contained in a system A can be measured by Eq. (15) and is known as Shannon's entropy $S(A)$.

$$S(A) = -\sum_{i=1}^{E} p_i \ ln\ p_i \tag{15}$$

where, E is the number of events with p_i probabilities. Renyi (1961) extended the Shannon entropy to define the Rényi entropy (R) according to Eq. (16).

$$R_\alpha(A) = \frac{1}{1-\alpha} ln \sum_{i=1}^{E} p_i^\alpha \tag{16}$$

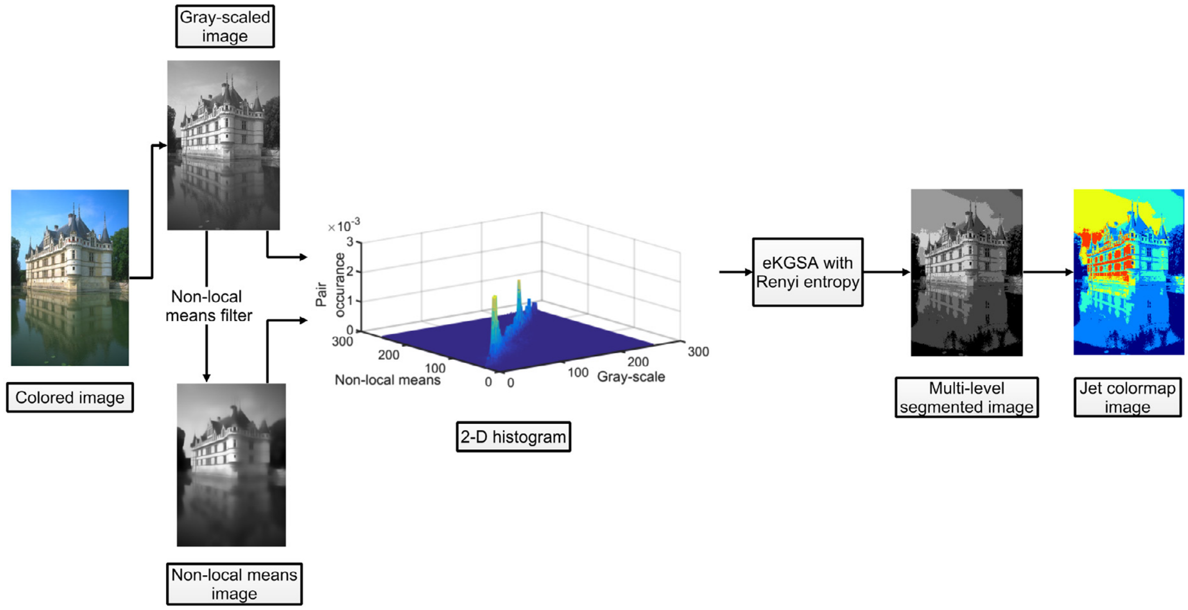

Fig. 1. Flow chart of the proposed image segmentation method (2DNLMeKGSA).

where, $\alpha \neq 1$ is an arbitrary positive real number and is known as the order of the entropy.

3. Proposed image thresholding segmentation method

The flow graph of the proposed two-dimensional non-local means exponential $Kbest$ gravitational search algorithm (2DNLMeKGSA) for multi-level image thresholding segmentation is illustrated in Fig. 1. As shown in Fig. 1, the input image is first converted into a gray-scale image followed by its non-local means filtered image. The gray-scale and non-local means filtered images are used to compute the proposed 2D histogram. The generated 2D histogram is further given to the novel eKGSA to obtain multi-level thresholds using modified Rényi entropy as an objective function. The obtained thresholds are used to segment the image into a number of regions. The descriptions of the proposed non-local means two dimensional histogram, exponential $Kbest$ gravitational search algorithm, and Rényi entropy are presented in the following sections. The steps of proposed 2DNLMeKGSA are presented in Algorithm 2.

Algorithm 2 Proposed Image Segmentation Method (2DNLMeKGSA)

Input: Let X is a gray scale image of size $U \times V$.
Output: Segmented image having n number of sub-regions.

1: Compute an image Y by applying non-local means filter on X
2: Generate non-local means based 2D histogram by using Eq. (17)
3: Randomly initialize population N of $2 * (n-1)$ dimensions. Each individual contains $(n-1)$ gray level thresholds, $\{t_1, t_2, \ldots, t_{n-1}\}$ and $(n-1)$ non-local means thresholds, $\{s_1, s_2, \ldots, s_{n-1}\}$.
4: Set $Kbest = N$
5: Evaluate the fitness fit of each individual of N by using multilevel Rényi entropy on 2D histogram according to Eq. (20).
6: Run eKGSA on the initialized N and its fitness values as per Algorithm 3
7: Use the optimal gray level thresholds, $\{t_1, t_2, \ldots, t_{n-1}\}$, generated by eKGSA to segment the image into n sub-regions.

3.1. Non-local means two dimensional histogram

Abutaleb (1989) introduced the concept of a 2D histogram to solve the image segmentation problem. For the same, they defined 2D histogram by mapping gray level of pixels with the corresponding local mean of neighboring pixels. However, considering local mean in 2D histogram computation leads to the loss of fine details of an image such as points, lines, and edges (Buades et al., 2005). Therefore, in this paper, the local mean filter is replaced by the non-local means filter which shows greater post-filtering clarity. Non-local means filter, as described in Section 2.1, computes the mean of all pixels in the image, weighted by the similarity of the pixels with the target pixel (Buades et al., 2005).

Let $f(x, y)$ represents the gray level ([0–L–1]) of a pixel at spatial coordinate (x, y) in an image of size $U \times V$. The $g(x, y)$ corresponds to the non-local means value of the pixel at (x, y), generated by applying the non-local means filter as described in Section 2.1. The 2D histogram is calculated by Eq. (17) using an input image and its non-local means filtered image and is illustrated in Fig. 2.

$$h(i, j) = c_{ij} \tag{17}$$

where, $i = f(x, y)$, $j = g(x, y)$, and c_{ij} represents the occurrence of the pair (i, j). In Fig. 2, horizontal and vertical axes represent the pixel values of input image $f(x, y)$ and pixel values of its non-local means filtered image $g(x, y)$ respectively. The intervals of each axis are defined by the corresponding threshold levels of the images. Each quadrant contains the frequency occurrence of the pair $f(x, y)$ and $g(x, y)$. Furthermore, the diagonal quadrants are specified by numbers $\{1, 2, \ldots, n\}$, whereas, other quadrants are not enumerated. From the above constructed 2D histogram (h), the normalized histogram is calculated as per Eq. (18).

$$P_{ij} = \frac{c_{ij}}{U \times V} \tag{18}$$

To visualize the 2D histogram, Fig. 3 shows two randomly selected images from BSDS300 and their respective 2D histograms. From the figure, it is evident that the information of objects and background is available along the diagonal of the plane while off-diagonal elements show edges and noise information. However, the main target of the proposed method is to segment objects from the background, thus only diagonal regions are considered while the off-diagonal regions are ignored.

3.2. Exponential Kbest gravitational search algorithm (eKGSA)

A well-found equilibrium between exploration and exploitation ascertains the success of a meta-heuristic algorithm (Feoktistov, 2006). In GSA, $Kbest$ function regulates this trade-off and determines the number of objects applying gravitational force in the system. This function

(a) Bears: Image.

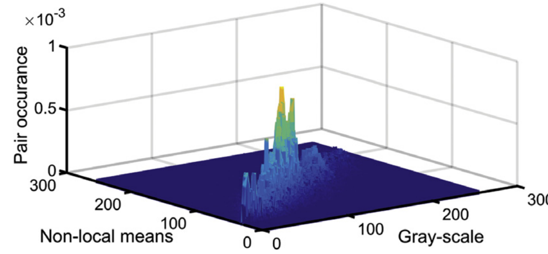

(b) Bears: 2D histogram.

(c) Bird: Image.

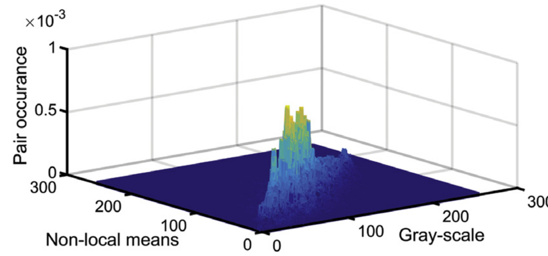

(d) Bird: 2D histogram.

Fig. 3. Three dimensional view of 2D histograms of Bear and Bird images taken from BSDS300.

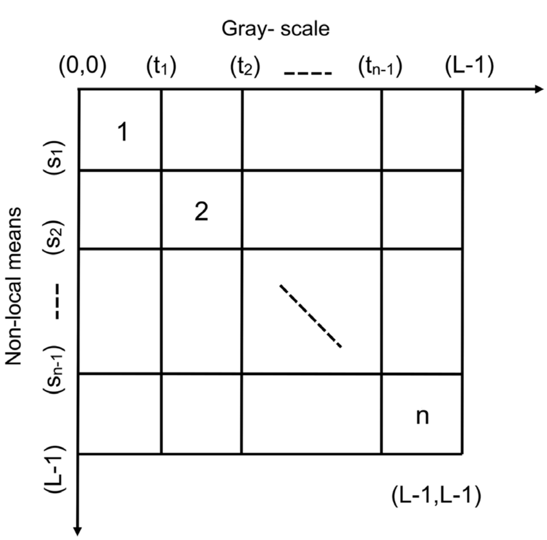

Fig. 2. Two Dimensional (2D) histogram.

reduces linearly with the increase of iterations. In the proposed eKGSA, a novel exponentially decreasing $Kbest$ is defined by Eq. (19).

$$Kbest(t) = \left(\frac{final\_per}{N}\right)^{\frac{t}{max\_it}} \tag{19}$$

where, max_it is the maximum number of iterations, N is the number of objects, t is the current iteration, and $final\_per$ is the percent of objects applying force on others at an iteration t. The values of exponential $Kbest$ at different iterations are depicted in Fig. 4 for $N = 50$ and $max\_it = 1000$. As evident from the figure, the $Kbest$ function is decreasing exponentially that makes the proposed eKGSA to perform good exploration at the initial stage followed by exhaustive exploitation at the later stage i.e., exploration is followed by exploitation with more number of iterations. The pseudocode of the proposed eKGSA is presented in Algorithm 3.

Algorithm 3 Exponential $Kbest$ Gravitational Search Algorithm (eKGSA)

Input: N objects having u dimensions. Assume the value of $final\_per$.
Output: The best solution having the heaviest mass.

```
Randomly initialize the initial population of N objects;
Evaluate the fitness fit of each object;
Compute the mass M of each object by Eq. (10);
Set Kbest = N;
while stopping criteria is not satisfied do
    Compute the acceleration a of each object by Eq. (8);
    Compute the velocity v of each object by Eq. (13);
    Update the position of each object by Eq. (14);
    Evaluate the fitness fit for each object;
    Compute the mass M of each object by Eq. (10);
    Update Kbest as: Kbest = (final_per / N)^(t / max_it),
end while
```

Furthermore, the proposed eKGSA is used for segmenting an image into different regions by finding the optimal thresholds. To divide an image into n regions, $(n-1)$ thresholds are calculated by the proposed eKGSA. However, the fitness value in eKGSA is computed by the proposed Rényi entropy which is described in the following section.

3.3. Rényi entropy for multi-level thresholded 2D histogram

Rényi entropy is a measure of information within a specific region. With respect to 2D histogram, it has only been applied for bi-level thresholding. In this paper, Rényi entropy (Renyi, 1961) for bi-level 2D histogram proposed by Sahoo and Arora (2004) has been generalized for the multi-level thresholded 2D histogram. For the same, the 2D histogram is subdivided into n^2 sub-regions as shown in Fig. 2, where the division is made on the basis of number of gray-level thresholds $\{t_1, t_2, \ldots, t_{n-1}\}$ and non-local means thresholds $\{s_1, s_2, \ldots, s_{n-1}\}$. Among the n^2 possible sub-regions, only diagonal sub-regions are considered since they contain maximum information of the image as apparent from Fig. 3 and are numbered as $\{1, 2, \ldots, n\}$ in Fig. 2. These diagonal sub-regions are used to calculate the Rényi entropy for positive $\alpha \neq 1$, as

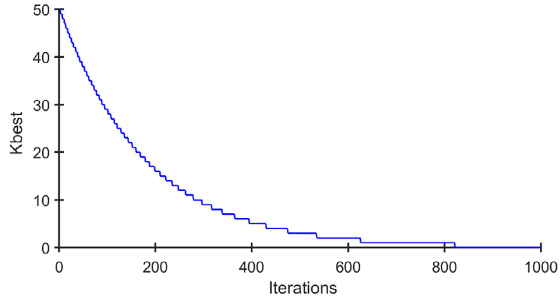

Fig. 4. Exponential *Kbest* over iterations.

depicted in Eq. (20).

$$H^{\alpha}(t,s)=\sum_{k=1}^{n-1}H_k^{\alpha}(t_k,s_k) \tag{20}$$

where, $H_k^{\alpha}(t_k,s_k)$ is Rényi entropy of k^{th} diagonal sub-region $\{k = 1,2,\dots,n\}$ bounded by (t_k,s_k) and is defined by Eq. (21).

$$H_k^{\alpha}(t_k,s_k)=\frac{1}{1-\alpha}ln\sum_{i=t_{k-1}+1}^{t_k}\sum_{j=s_{k-1}+1}^{s_k}\left(\frac{P_{ij}}{P_k}\right)^{\alpha} \tag{21}$$

where, P_{ij} is the value of normalized 2D histogram at (i,j) location and P_k represents the total sum of values at k^{th} diagonal sub-region in normalized 2D histogram as shown in Eq. (22).

$$P_k=\sum_{i=t_{k-1}+1}^{t_k}\sum_{j=s_{k-1}+1}^{s_k}P_{ij} \tag{22}$$

Therefore, in this paper, $eKGSA$ uses the redefined Rényi entropy as an objective function which is maximized to obtain the optimal set of multi-level thresholds $\{t_1,t_2,\dots,t_{n-1}\}$ i.e.,

$$Maximize: \; H^{\alpha}(t,s); \quad for\; t,s\in[0,L-1] \tag{23}$$

4. Experimental results

4.1. Experimental setup and database

The experiments have been simulated on a computer of 2.80 GHz Intel® core i3 processor and 2 GB of RAM using Matlab 2015a. The analysis has been done on 300 images of Berkeley Segmentation Dataset and Benchmark (BSDS300) (The Berkeley Segmentation Dataset and Benchmark, 2017). In BSDS300, each image is provided with a set of ground truth images, compiled by human observers. The size of all images is 481 × 321 pixels. However, each image is normalized with the longest side as 320 pixels. The optimal multi-level thresholds in the proposed 2D non-local means (2DNLM) image segmentation method are calculated using the proposed eKGSA and the other existing meta-heuristics namely; cKGSA, GSA, ABC, and DE. The parameter settings of eKGSA algorithm is listed in Table 1. Each meta-heuristic algorithm is executed 30 times to minimize the interference.

4.2. Performance evaluation parameters

The performance of the proposed method has been evaluated in perspective of objective and subjective assessments. Two random images from BSDS300 along with the corresponding segmented images returned by each algorithm have been considered in this paper for subjective analysis. For objective assessment, twelve image segmentation performance parameters are used and briefed in Table 2 along with their formulations.

In Table 2, BDE, PRI, VoI, and GCE are the statistical measures to represent the quality of a segmented image (Yang et al., 2008; Sathya and Manavalan, 2011; Unnikrishnan et al., 2007). SSIM and FSIM predict the perceived image quality and statistically validate the consistency of the segmentation results with the results of the human observers (Wang et al., 2004; Zhang et al., 2011; Sasivarnan and Jagan, 2011). Furthermore, RMSE, PSNR, NCC, AD, MD, and NAE are the full reference image quality measures based on statistical error and correlation (Sasivarnan and Jagan, 2011; Lewis, 1995). SSIM, FSIM, RMSE, PSNR, NCC, AD, MD, and NAE use pixel information (Sasivarnan and Jagan, 2011) while in BDE, PRI, VoI, and GCE, labeling information of the pixels is used (Sathya and Manavalan, 2011; Unnikrishnan et al., 2007). Moreover, PRI, SSIM, FSIM, PSNR, and NCC show better segmentation for higher side values while for other performance parameters, lower side values are better (Sarkar and Das, 2013; Zhao et al., 2016; Panda et al., 2017; Sasivarnan and Jagan, 2011; Singh et al., 2012).

Table 1
Parameter settings for eKGSA.

Parameter	eKGSA
Population size (N)	50
Number of iterations (max_it)	1000
Gconstant (G_0)	100
Beta (β)	20
$final\_per$	2

4.3. Experimental analyses of the proposed method

In the proposed method, α defines the order of entropy in Rényi entropy. The effect of this parameter on the proposed method is studied empirically on the twelve performance parameters, mentioned in Table 2, for 3-level image thresholding segmentation on BSDS300 over different values of α, where $\alpha \in (0,1.5]$, $\alpha \neq 1$. It is observed that the performance is consistent for $\alpha \in [0.1,0.9]$ and abruptly degrades over $\alpha > 1$. Thus, it is reasonable to take the value of α in the range [0.1, 0.9]. In this paper, the value of α is set to 0.45.

The proposed method uses the non-local means 2D histogram in place of the local mean 2D histogram (Abutaleb, 1989). Fig. 5 depicts the effect of non-local means and local mean on an image. It is visualized that loss of the fine details in a non-local means filtered image is much less than a local mean filtered image.

The proposed eKGSA is used to find the optimal thresholds for image segmentation. For the same, modified Rényi entropy is used as an objective function. The performance of eKGSA has been compared with four existing meta-heuristic algorithms namely; cKGSA, GSA, ABC, and DE, in terms of convergence behavior as shown in Fig. 6 for 3-level and 5-level image thresholding segmentations. The convergence graphs have been plotted between the best fitness value and the number of iterations in logarithmic scale on a randomly chosen image from BSDS300. From Fig. 6, it is observed that initially eKGSA converges gradually, which represents its exploration capability and finally reaches to an optimum. Moreover, the convergence towards optimum is comparatively faster than other considered meta-heuristic algorithms. Thus, the results elicit that the proposed eKGSA outperforms the other existing meta-heuristic algorithms.

Fig. 7 illustrates the subjective analysis of the proposed and the considered methods for 3-level and 5-level image thresholding segmentations on two representative images (mountains and giraffes). The figure depicts the original images, corresponding human segmented images (Ground Truth) and the segmented images returned by 2DNLMcKGSA, 2DNLMGSA, 2DNLMDE, 2DNLMABC, and 2DNLMeKGSA methods. It can be discerned from Fig. 7 that the proposed method returns fine-detailed segmented images as compared to existing methods for both 3-level and 5-level image thresholding segmentations. In Fig. 7(a), the proposed method clearly segments the sky from mountains while other considered methods fail to do so. Likewise, in Fig. 7(c), 2DNLMeKGSA returns fine edges around clouds and mountains for 5-level segmentation. Similarly, in Fig. 7(b)–(d), the 2DNLMeKGSA is able to separate the

Table 2
Performance parameters considered for evaluation of the proposed method with the other considered methods for multi-level image thresholding segmentation.

S. No.	Parameters	Formulation	Remark
1.	Boundary Displacement Error (BDE) (Yang et al., 2008; Sathya and Manavalan, 2011)	$\text{BDE} = \begin{cases} \frac{u-v}{L-1}, & 0 < (u-v) \\ 0, & (u-v) < 0 \end{cases}$	Computes the displacement error of the boundary pixels between two segmented images.
2.	Probability Rand Index (PRI) (Yang et al., 2008; Sathya and Manavalan, 2011)	$\text{PRI} = \frac{a+b}{a+b+c+d} = \frac{a+b}{L}$	Finds the labeling consistency between the segmented image and its ground truth.
3.	Variation of Information (VoI) (Yang et al., 2008; Sathya and Manavalan, 2011)	$\text{VoI} = H(S_1) + H(S_2) - 2I(S_1, S_2)$	Determines the randomness in one segmentation from given segmentation in terms of distance.
4.	Global Consistency Error (GCE) (Yang et al., 2008; Sathya and Manavalan, 2011)	$\text{GCE} = \frac{1}{n}\left\{\sum_i E(S_1, S_2, p_i), \sum_i E(S_2, S_1, p_i)\right\}$	Measures the refinement in one segmentation over the other.
5.	Structural Similarity Index (SSIM) (Wang et al., 2004)	$\text{SSIM} = \frac{(2\times\bar{X}\times\bar{Y}+c_1)(2\times\sigma_{XY}+c_2)}{(\sigma_X^2+\sigma_Y^2+c_2)\times((\bar{X})^2+(\bar{Y})^2+c_1)}$	Finds the similarity between segmented image and uncompressed or distortion-free image.
6.	Feature Similarity Index (FSIM) (Zhang et al., 2011)	$\text{FSIM} = \frac{\sum_{x\in\Omega} S_L(x).PC_m(x)}{\sum_{x\in\Omega} PC_m(x)}$	Defines the quality score which reflects the significance of a local structure.
7.	Root Mean Squared Error (RMSE) (Hyndman and Koehler, 2006; Sasivarnan and Jagan, 2011)	$\text{RMSE} = \sqrt{\text{MSE}(\hat{\theta})} = \sqrt{\text{E}((\hat{\theta}-\theta)^2)}$	Computes the difference between the predicted value, given by a model or an estimator, and the actual value.
8.	Peak Signal to Noise Ratio (PSNR) (Sasivarnan and Jagan, 2011; Huynh-Thu and Ghanbari, 2008)	$\text{PSNR} = 10log_{10}\frac{(2^b-1)^2}{\sqrt{\text{MSE}}}$	Represents the ratio between the maximum possible power of a signal and the power of corrupting noise.
9.	Normalized Cross-Correlation (NCC) (Lewis, 1995)	$\text{NCC} = \frac{1}{n}\sum_{x,y}\frac{1}{\sigma_X\sigma_Y}\left(X(x,y)-\bar{X}\right)\left(Y(x,y)-\bar{Y}\right)$	Used for template matching, where images are first normalized due to lighting and exposure conditions.
10.	Average Difference (AD) (Sasivarnan and Jagan, 2011; Eskicioglu and Fisher, 1995)	$\text{AD} = \frac{1}{MN}\sum_{x=1}^{M}\sum_{y=1}^{N}(X(x,y)-Y(x,y))$	Calculates the average difference between the pixel values.
11.	Maximum Difference (MD) (Sasivarnan and Jagan, 2011; Eskicioglu and Fisher, 1995)	$\text{MD} = max \lvert X(x,y)-Y(x,y) \rvert$	Determines the maximum error signal by taking the difference between original image and segmented image.
12.	Normalized Absolute Error (NAE) (Sasivarnan and Jagan, 2011; Singh et al., 2012)	$\text{NAE} = \frac{\sum_{x=1}^{M}\sum_{y=1}^{N}\lvert X(x,y)-Y(x,y)\rvert}{\sum_{x=1}^{M}\sum_{y=1}^{N}\lvert X(x,y)\rvert}$	Computes the normalized absolute difference between the original and corresponding segmented images.

(a) Original image.

(b) Non-local means filtered image.

(c) Local mean filtered image.

Fig. 5. Comparison of non-local means and local mean on an image.

clouds with clear edges as compared to other methods for both levels of image segmentation. Thus, it is inferred from the subjective comparison that proposed 2DNLMeKGSA has surpassed the considered methods for multi-level image thresholding segmentation.

Moreover, the objective performance of the proposed image thresholding segmentation method is done using twelve evaluation parameters as presented in Table 2. Tables 3–4 show the average values of each considered parameter on 300 images of BSDS300 for 3-level and 5-level

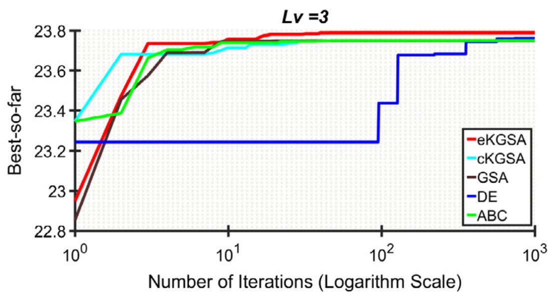

(a) 3-Level segmentation.

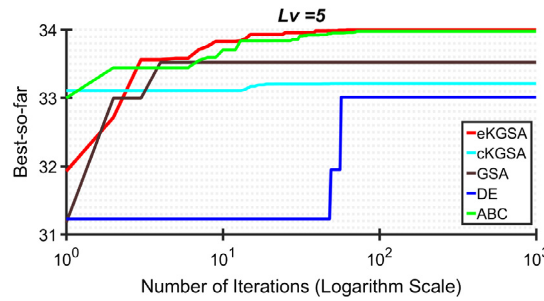

(b) 5-level segmentation.

Fig. 6. The convergence performance of eKGSA, cKGSA, GSA, DE, and ABC meta-heuristic algorithms.

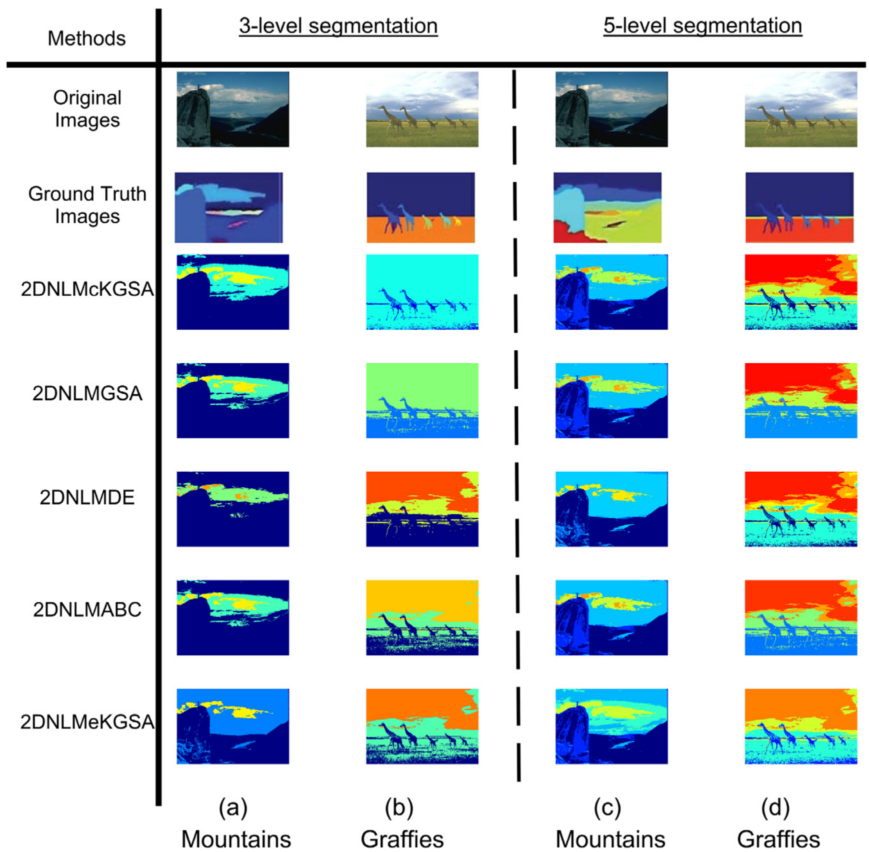

Fig. 7. Subjective analysis of multi-level image thresholding segmentation methods at 3-level and 5-level.

Table 3
Performance comparison of the proposed method with the other considered methods for BSDS300 with 3-level image thresholding segmentation.

Parameters	2DNLMcKGSA	2DNLMGSA	2DNLMDE	2DNLMABC	2DNLMeKGSA
BDE	10.2719	10.2567	10.4560	10.4109	**10.2407**
PRI	0.6070	0.6073	0.6016	0.5993	**0.6079**
VoI	2.8060	2.8067	**2.7828**	2.7882	2.8078
GCE	0.3345	0.3348	0.3247	**0.3238**	0.3352
SSIM	0.4529	0.4529	0.4423	0.4398	**0.4549**
FSIM	0.6742	**0.6749**	0.6697	0.6691	0.6747
RSME	50.0259	50.0514	51.1517	51.7063	**49.8913**
PSNR	14.4092	14.4014	14.2079	14.1617	**14.4306**
NCC	0.6517	0.6517	0.6414	0.6369	**0.6532**
AD	42.7141	42.7436	43.7985	44.2451	**42.5637**
MD	110.9258	110.9021	111.1072	113.7159	**110.8570**
NAE	0.4099	0.4100	0.4220	0.4257	**0.4080**

Table 4
Performance comparison of the proposed method with the other considered methods for BSDS300 with 5-level image thresholding segmentation.

Parameters	2DNLMcKGSA	2DNLMGSA	2DNLMDE	2DNLMABC	2DNLMeKGSA
BDE	9.8978	9.9448	10.0865	9.9355	**9.8776**
PRI	0.7010	0.6610	0.6450	0.6553	**0.7261**
VoI	3.1419	3.1415	**3.0676**	3.1283	3.1436
GCE	0.4391	0.4396	**0.4124**	0.4332	0.4397
SSIM	0.6569	0.6566	0.5980	0.6428	**0.6582**
FSIM	0.7858	0.7857	0.7549	0.7808	**0.7863**
RSME	29.4240	**29.3868**	35.1074	30.9452	29.3922
PSNR	18.9410	**18.9516**	17.5650	18.5960	18.9463
NCC	0.8004	0.8006	0.7629	0.7888	**0.8008**
AD	24.9601	24.9333	29.4665	26.1351	**24.8999**
MD	69.8932	**69.5218**	79.7659	73.2606	70.1836
NAE	0.2420	0.2419	0.2878	0.2557	**0.2412**

image segmentations respectively. From Tables 3–4, it is observed that 2DNLMeKGSA method has BDE value of 10.2407 and 9.8776 for 3-level and 5-level segmentations respectively which are the lowest values among the considered methods. This reflects the minimum deviation between the segmented image and its ground truth image and can also be visualized in Fig. 7. The proposed method also returns the maximum values for PRI i.e., 0.6079 and 0.7261, for 3-level and 5-level segmentations respectively, which indicates the best segmentation consistency. However, for VoI and GCE parameters, 2DNLMeKGSA method has competitive results.

In 3-level segmentation, the proposed method achieves maximal value for SSIM (0.4549) and substantial value for FSIM (0.6747) as compared to other considered methods. However, in 5-level segmentation, the proposed method returns superior values for both SSIM and FSIM parameters i.e., 0.6582 and 0.7863 respectively. As both SSIM and FSIM are the indicators of the perceived image quality (Zhang et al., 2011), it is pertinent to state that the evaluation results are statistically consistent with those of human observers. Likewise, for the statistical error parameters (RMSE, AD, MD, and NAE), the proposed 2DNLMeKGSA method has attained minimum values in 3-level segmentation. For 5-level segmentation, AD and NAE values are minimized while equitable values of RMSE and MD are returned by 2DNLMeKGSA. As PSNR and RMSE are inversely proportional, the obtained results for all the methods are justifiable for both levels of segmentation. Further, the obtained cross-correlation (NCC) values for 3-level and 5-level segmentations are 0.6532 and 0.8008 respectively which are the highest among the considered methods. Thus, from Tables 3–4, it is affirmed that the proposed method yields superior segmentation results than the other considered methods and can serve as a useful alternative in multi-level image thresholding segmentation.

5. Conclusion

In this paper, a novel multi-level image thresholding segmentation method has been proposed. The presented method has four folds, (i) Non-local means based 2D histogram is defined, (ii) An efficient variant of gravitational search algorithm called exponential $Kbest$ gravitational search algorithm (eKGSA) has been introduced, (iii) Rényi entropy is redefined for multi-level 2D histogram, (iv) A novel method, two-dimensional non-local means exponential $Kbest$ gravitational search algorithm (2DNLMeKGSA), for multi-level image thresholding segmentation has been proposed. The experiments are conducted on Berkeley Segmentation Dataset and Benchmark (BSDS300) for subjective as well as objective assessments on 3-level and 5-level image thresholding segmentations. The objective analysis is done on 12 state-of-the-art measures and compared with four methods namely; 2DNLMcKGSA, 2DNLMGSA, 2DNLMDE, and 2DNLMABC.

From the experimental results, it has been observed that the proposed non-local means based 2D histogram retains the fine details in the filtered image as compared to local mean based 2D histogram. The effectiveness of the newly introduced eKGSA has been studied in terms of convergence behavior which uses redefined Rényi entropy as an objective function for extracting optimal thresholds in the proposed 2DNLMeKGSA method. The subjective analysis of 2DNLMeKGSA method exhibits more promising results than the existing methods. Likewise, the experimental results of the objective analysis revealed that the proposed method has better values on the maximum number of performance measures. Thus it can be concluded that the proposed method outperforms the existing compared methods for multi-level image thresholding segmentation.

Moreover, determining multi-level thresholds for image segmentation is an NP-hard combinatorial optimization problem for a large number of thresholds and requires $O(L^{n-1})$ computational complexity for $(n-1)$ thresholds in case of an exhaustive search (Ishak, 2017; Nakib et al., 2010; Sarkar et al., 2016). Clearly, it will grow exponentially as the number of thresholds increase. Therefore, the proposed method reduces the aforesaid complexity by using eKGSA for finding multi-level thresholds. In the worst case scenario of eKGSA, each object applies force on every other object. Hence, the computational complexity of eKGSA is $O(N^2)$, where N is the population size. Thus, the proposed method will be effective to segment the images in the reasonable amount of time.

In future, the proposed work may be extended to compute the thresholding levels automatically according to the properties of an image. Further, it may be parallelized to reduce the computational complexity for high dimensional datasets. Apart from this, other objective functions such as fuzzy entropy could be explored to enhance the efficiency. The applicability of the proposed method may be tested for different real-time applications such as pedestrian detection, nuclei detection, and satellite image segmentation.

References

Abutaleb, A.S., 1989. Automatic thresholding of gray-level pictures using two-dimensional entropy. Comput. Vis. Graph. Image Process. 47, 22–32.
Akay, B., 2013. A study on particle swarm optimization and artificial bee colony algorithms for multilevel thresholding. Appl. Soft Comput. 13, 3066–3091.
Albuquerque, M.P.D., Esquef, I.A., Mello, A.G., 2004. Image thresholding using tsallis entropy. Pattern Recognit. Lett. 25, 1059–1065.
Arbelaez, P., Maire, M., Fowlkes, C., Malik, J., 2011. Contour detection and hierarchical image segmentation. IEEE Trans. Pattern Anal. Mach. Intell. 33, 898–916.
Bekenstein, J.D., 1973. Black holes and entropy. Phys. Rev. D 7, 23–33.
Boccaletti, S., Grebogi, C., Lai, Y.-C., Mancini, H., Maza, D., 2000. The control of chaos: Theory and applications. Phys. Rep. 329, 103–197.
Brink, A., 1992. Thresholding of digital images using two-dimensional entropies. Pattern Recognit. 25, 803–808.
Buades, A., Coll, B., Morel, J.-M., 2005. A non-local algorithm for image denoising. In: Proc. of IEEE Computer Society Conference on Computer Vision and Pattern Recognition.
Chatterjee, A., Ghoshal, S., Mukherjee, V., 2012. A maiden application of gravitational search algorithm with wavelet mutation for the solution of economic load dispatch problems. Int. J. Bio-Inspired Comput. 4, 33–46.
Cheng, H., Chen, Y., Jiang, X., 2000. Thresholding using two-dimensional histogram and fuzzy entropy principle. IEEE Trans. Image Process. 9, 732–735.
Cheng, C., Hao, X., Liu, S., 2014. Image segmentation based on 2d renyi gray entropy and fuzzy clustering. In: Proc. of International Conference on Signal Processing.

Cheng, H.-D., Jiang, X., Wang, J., 2002. Color image segmentation based on homogram thresholding and region merging. Pattern Recognit. 35, 373–393.

Dirami, A., Hammouche, K., Diaf, M., Siarry, P., 2013. Fast multilevel thresholding for image segmentation through a multiphase level set method. Signal Process. 93, 139–153.

Eskicioglu, A.M., Fisher, P.S., 1995. Image quality measures and their performance. IEEE Trans. Commun. 43, 2959–2965.

Felzenszwalb, P.F., Huttenlocher, D.P., 2004. Efficient graph-based image segmentation. Int. J. Comput. Vis. 59, 167–181.

Fengjie, S., He, W., Jieqing, F., 2009. 2d otsu segmentation algorithm based on simulated annealing genetic algorithm for iced-cable images. In: Proc. of International Forum on Information Technology and Applications.

Feoktistov, V., 2006. Differential Evolution. Springer.

Goossens, B., Luong, Q., Pizurica, A., Philips, W., 2008. An improved non-local denoising algorithm. In: Proc. of International Workshop on Local and Non-Local Approximation in Image Processing.

Han, X., Chang, X., 2012. A chaotic digital secure communication based on a modified gravitational search algorithm filter. Inform. Sci. 208, 14–27.

Han, Y., Feng, X.-C., Baciu, G., 2013. Variational and pca based natural image segmentation. Pattern Recognit. 46, 1971–1984.

Huynh-Thu, Q., Ghanbari, M., 2008. Scope of validity of psnr in image/video quality assessment. Electron. Lett. 44, 800–801.

Hyndman, R.J., Koehler, A.B., 2006. Another look at measures of forecast accuracy. Int. J. Forecast. 22, 679–688.

Ishak, A.B., 2017. Choosing parameters for rényi and tsallis entropies within a two-dimensional multilevel image segmentation framework. Physica A 466, 521–536.

Kapur, J.N., Sahoo, P.K., Wong, A.K., 1985. A new method for gray-level picture thresholding using the entropy of the histogram. Comput. Vis. Graph. Image Process. 29, 273–285.

Krinidis, M., Pitas, I., 2009. Color texture segmentation based on the modal energy of deformable surfaces. IEEE Trans. Image Process. 18, 1613–1622.

Kumar, S., Sharma, T.K., Pant, M., Ray, A., 2012. Adaptive artificial bee colony for segmentation of ct lung images. In: Proc. of International Conference on Recent Advances and Future Trends in Information Technology. 2012.

Kumar, Y., Sahoo, G., 2014. A review on gravitational search algorithm and its applications to data clustering & classification. Int. J. Intell. Syst. Appl. 6, 79–93.

Lei, X., Fu, A., 2008. Two-dimensional maximum entropy image segmentation method based on quantum-behaved particle swarm optimization algorithm. In: Proc. of International Conference on Natural Computation.

Lewis, J.P., 1995. Fast normalized cross-correlation. Proc. Vis. Interface 10, 120–123.

Li, C., Li, H., Kou, P., 2014. Piecewise function based gravitational search algorithm and its application on parameter identification of avr system. Neurocomputing 124, 139–148.

Li, C., Tam, P.K.-S., 1998. An iterative algorithm for minimum cross entropy thresholding. Pattern Recognit. Lett. 19, 771–776.

Marciniak, A., Kowal, M., Filipczuk, P., Korbicz, J., 2014. Swarm intelligence algorithms for multi-level image thresholding. In: Proc. of Intelligent Systems in Technical and Medical Diagnostics.

Mignotte, M., 2010. A label field fusion bayesian model and its penalized maximum rand estimator for image segmentation. IEEE Trans. Image Process. 19, 1610–1624.

Mittal, H., Pal, R., Kulhari, A., Saraswat, M., 2016. Chaotic *Kbest* gravitational search algorithm (ckgsa). In: Proc. of International Conference on Contemporary Computing.

Nakib, A., Oulhadj, H., Siarry, P., 2010. Image thresholding based on pareto multiobjective optimization. Eng. Appl. Artif. Intell. 23, 313–320.

Nakib, A., Roman, S., Oulhadj, H., Siarry, P., 2007. Fast brain mri segmentation based on two-dimensional survival exponential entropy and particle swarm optimization. In: Proc. of International Conference on Engineering in Medicine and Biology Society.

Nie, F., 2015. Tsallis cross-entropy based framework for image segmentation with histogram thresholding. J. Electron. Imaging 24, 013002–013002.

Otsu, N., 1979. A threshold selection method from gray-level histograms. IEEE Trans. Syst. Man Cybern. 9, 62–66.

Pal, K., Saha, C., Das, S., Coello, C.A.C., 2013. Dynamic constrained optimization with offspring repair based gravitational search algorithm. In: Proc. of IEEE congress on Evolutionary computation.

Panda, R., Agrawal, S., Samantaray, L., Abraham, A., 2017. An evolutionary gray gradient algorithm for multilevel thresholding of brain mr images using soft computing techniques. Appl. Soft Comput. 50, 94–108.

Qi, C., 2014. Maximum entropy for image segmentation based on an adaptive particle swarm optimization. Appl. Math. 8, 3129–3135.

Rashedi, E., Nezamabadi-Pour, H., Saryazdi, S., 2009. Gsa: A gravitational search algorithm. Inform. Sci. 179, 2232–2248.

Renyi, A., 1961. On measures of entropy and information. In: Proc. of Berkeley symposium on mathematical statistics and probability.

Sahoo, P.K., Arora, G., 2004. A thresholding method based on two-dimensional renyi's entropy. Pattern Recognit. 37, 1149–1161.

Sahoo, P.K., Arora, G., 2006. Image thresholding using two-dimensional tsallis–havrda–charvát entropy. Pattern Recognit. Lett. 27, 520–528.

Sahoo, P., Wilkins, C., Yeager, J., 1997. Threshold selection using renyi's entropy. Pattern Recognit. 30, 71–84.

Sarkar, S., Das, S., 2013. Multilevel image thresholding based on 2d histogram and maximum tsallis entropy—a differential evolution approach. IEEE Trans. Image Process. 22, 4788–4797.

Sarkar, S., Das, S., Chaudhuri, S.S., 2015. A multilevel color image thresholding scheme based on minimum cross entropy and differential evolution. Pattern Recognit. Lett. 54, 27–35.

Sarkar, S., Das, S., Chaudhuri, S.S., 2016. Hyper-spectral image segmentation using rényi entropy based multi-level thresholding aided with differential evolution. Expert Syst. Appl. 50, 120–129.

Sasivarnan, K.J.J.D.R.D.C., Jagan, A., 2011. Image quality assessment techniques in spatial domain. Int. J. Comput. Sci. Technol. 2, 77–81.

Sathya, B., Manavalan, R., 2011. Image segmentation by clustering methods: Performance analysis. Int. J. Comput. Appl. 29, 0975–8887.

Sezgin, M., et al., 2004. Survey over image thresholding techniques and quantitative performance evaluation. J. Electron. Imaging 13, 146–168.

Sha, C., Hou, J., Cui, H., 2016. A robust 2d otsu's thresholding method in image segmentation. J. Vis. Commun. Image Represent. 41, 339–351.

Shannon, C.E., 2001. A mathematical theory of communication. ACM SIGMOBILE Mob. Comput. Commun. Rev. 5, 3–55.

Shen, X., Zhang, Y., Li, F., 2009. An improved two-dimensional entropic thresholding method based on ant colony genetic algorithm. In: Proc. of WRI Global Congress on Intelligent Systems.

Shi, J., Malik, J., 2000. Normalized cuts and image segmentation. IEEE Trans. Pattern Analysis Mach. Intell. 22, 888–905.

Singh, S., Bansal, R., Bansal, S., 2012. Comparative study and implementation of image processing techniques using matlab. Int. J. Adv. Res. Comput. Sci. Softw. Eng. 2, 37–44.

Tan, K.S., Isa, N.A.M., 2011. Color image segmentation using histogram thresholding–fuzzy c-means hybrid approach. Pattern Recognit. 44, 1–15.

Tang, Y.-g., Liu, D., Guan, X.-p., 2007. Fast image segmentation based on particle swarm optimization and two-dimension otsu method. Control Decis. 22, 202–205.

Tian, Y., Li, J., Yu, S., Huang, T., 2015. Learning complementary saliency priors for foreground object segmentation in complex scenes. Int. J. Comput. Vis. 111, 153–170.

The berkeley segmentation dataset and benchmark, https://www2.eecs.berkeley.edu/Research/Projects/CS/vision/bsds/, accessed on 07/27/2017.

Tsai, H.-C., Tyan, Y.-Y., Wu, Y.-W., Lin, Y.-H., 2013. Gravitational particle swarm. Appl. Math. Comput. 219, 9106–9117.

Unnikrishnan, R., Pantofaru, C., Hebert, M., 2007. Toward objective evaluation of image segmentation algorithms. IEEE Trans. Pattern Anal. Mach. Intell. 29, 929–944.

Wang, Z., Bovik, A.C., Sheikh, H.R., Simoncelli, E.P., 2004. Image quality assessment: from error visibility to structural similarity. IEEE Trans. Image Process. 13, 600–612.

Wolpert, D.H., Macready, W.G., 1997. No free lunch theorems for optimization. IEEE Trans. Evolut. Comput. 1, 67–82.

Xiao-Feng, L., Hui-Ying, L., Ming, Y., Tai-Ping, W., 2016. Infrared image segmentation based on aafsa and 2d-renyi entropy threshold selection. In: Proc. of Joint International Conference on Artificial Intelligence and Computer Engineering and International Conference on Network and Communication Security. 2016.

Xue-guang, W., Shu-hong, C., 2012. An improved image segmentation algorithm based on two-dimensional otsu method. Inform. Sci. Lett. 1, 77–83.

Yang, A.Y., Wright, J., Ma, Y., Sastry, S.S., 2008. Unsupervised segmentation of natural images via lossy data compression. Comput. Vis. Image Underst. 110, 212–225.

Yang, X.-S., 2014. Nature-inspired Optimization Algorithms. Elsevier.

Yu, Z., Au, O.C., Zou, R., Yu, W., Tian, J., 2010. An adaptive unsupervised approach toward pixel clustering and color image segmentation. Pattern Recognit. 43, 1889–1906.

Zhang, H., Fritts, J.E., Goldman, S.A., 2008. Image segmentation evaluation: A survey of unsupervised methods. Comput. Vis. Image Underst. 110, 260–280.

Zhang, L., Zhang, L., Mou, X., Zhang, D., 2011. Fsim: A feature similarity index for image quality assessment. IEEE Trans. Image Process. 20, 2378–2386.

Zhang, X., Xu, C., Li, M., Sun, X., 2015. Sparse and low-rank coupling image segmentation model via nonconvex regularization. Int. J. Pattern Recognit. Artif. Intell. 29, 1–22.

Zhang, Y., Li, Y., Xia, F., Luo, Z., 2012. Immunity-based gravitational search algorithm. In: Proc. of International Conference on Information Computing and Applications.

Zhao, X., Turk, M., Li, W., K.-c. Lien, ., Wang, G., 2016. A multilevel image thresholding segmentation algorithm based on two-dimensional k–l divergence and modified particle swarm optimization. Appl. Soft Comput. 48, 151–159.